[4] Green, L., Jr., "Introductory Considerations of Hybrid Rocket Combustion," *Heterogeneous Combustion Progress in Aeronautics and Astronautics*, Vol. 15, Academic Press, New York, 1964, pp. 451–484.

[5] Tsugé, S. and Fujiwara, Y., "Fine Structure of Hybrid Combustion," *Astronautica Acta*, Vol. 14, 1969, pp. 327–335.

[6] Williams, F. A., *Combustion Theory*, Addison-Wesley, Reading, Pa., 1965.

[7] Liu, T. M. and Libby, P. A., "Boundary Layer at Stagnation Point with Hydrogen Injection," *Combustion and Science Technology*, Vol. 2, 1970, p. 131.

[8] Waldman, C. H., Cheng, S. I., Sirignano, W. A., and Summerfield, M., "Theoretical Studies of Diffusion Flame Structure," AFOSR Scientific Report 69-0350 TR, and AMS Report 860, 1969, Princeton Univ., Princeton, N.J.

[9] Chung, P. M., "Heat Transfer in Chemically Reacting Gases," *Advanced Heat Transfer*, edited by B. T. Chao, University of Illinois Press, Urbana, Ill., 1969, pp. 319–338.

[10] Penner, S. S. and Libby, P. A., "Convective Laminar Heat Transfer with Combustion for a Lewis Number of Unity," *Astronautica Acta*, Vol. 13, 1967, pp. 75–91.

[11] Kerzner, H., "Chemically Reacting Boundary Layer over a Vaporizing Surface," Ph.D. thesis, 1972, Univ. of Illinois, Urbana-Champaign, Ill.

[12] Libby, P. A. and Pierucci, M., "Laminar Boundary Layer with Hydrogen Injection Including Multicomponent Diffusion," *AIAA Journal*, Vol. 2, No. 12, Dec. 1964, pp. 2118–2126.

[13] Emmons, H. W., "Film Combustion of Liquid Fuels," *Zeitschrift für Agnewandte Mathematik und Mechanik*, Band 36, Heft 1/2, 1956, pp. 60–70.

[14] Chen, T. N. and Toong, T. Y., "Laminar Boundary Layer Wedge Flows with Evaporation and Combustion," *Heterogeneous Combustion Progress in Astronautics and Aeronautics*, Vol. 15, Academic Press, New York, 1964, pp. 643–664.

[15] Smoot, L. D. and Price, C. F., "Regression Rate of Mechanisms of Nonmetalized Hybrid Fuel Systems," *AIAA Journal*, Vol. 3, No. 8, Aug. 1965, pp. 1408–1413.

[16] Smoot, L. D. and Price, C. F., "Pressure Dependence of Hybrid Fuel Regression Rates," *AIAA Journal*, Vol. 5, No. 1, Jan. 1967, pp. 102–106.

[17] Kosdon, F. J. and Williams, F. A., "Pressure Dependence of Nonmetalized Hybrid Fuel Regression Rates," *AIAA Journal*, Vol. 5, No. 4, April 1967, pp. 774–778.

[18] Kumar, R. N. and Stickler, D. B., "Polymer-Degradation Theory for Pressure-Sensitive Hybrid Combustion," *Thirteenth Symposium on Combustion*, The Combustion Inst., Pittsburgh, Pa., 1970, pp. 1059–1072.

DECEMBER 1973 AIAA JOURNAL VOL. 11, NO. 12

Influence of Gradient of Velocity upon the Resonant Radiative Transfer in Plasma Flows

P. VALENTIN,* M. PINEGRE,† M. TERRIER‡
Commissariat à l'Energie Atomique, Sevran, France

The aim of this work is to estimate the influence of a velocity gradient upon the resonant radiative transfer and to propose an approximate analytical solution of the transfer equation. The radiative population rate of the resonant states is shown to be notably influenced by a velocity gradient of the same order as that found in a boundary layer along a wall in a supersonic flow. Thus this rate appears to be from one to three orders of magnitude smaller than in the case of zero gradient.

Nomenclature

A_{rf} = Einstein coefficient for spontaneous emission of the resonance lines
B = population rate due to the photons which are emitted in the freestream plasma
B_{fr} = Einstein coefficient for absorption
C = velocity of light
I_ν = specific intensity of the radiation at ν
k_ν = spectral absorption coefficient per unit length at ν
L = boundary-layer thickness
l = distance normal to the freestream boundary
l^* = dimensionless length (Sec. V)
L' = thickness of the plasma
$l' = L' - L$ = thickness of the homogeneous plasma
N = density number
S = line strength
U = velocity in the streamwise direction
u', v', w' = coordinate system (Fig. 4)
Z = distance normal to the wall
α = $(1/\delta\nu_D)^2$
β = expression defined in Eq. (10)
β_0 = value of β for zero gradient
β' = expression defined in Eq. (42)
γ = $|(1/C)\,\partial U/\partial Z|$
Δ = population rate due to the photons which are emitted in the nonhomogeneous plasma
$\delta\nu_D$ = (half) half-width doppler
θ, ϕ = angular coordinate system (Figs. 2 and 4)
ν = radiation frequency
ξ, η, ζ = coordinate system (Fig. 2)
τ = lifetime = $1/A_{rf}$
χ = dimensionless frequency

Subscripts
e = freestream value
f = ground state
m = metastable state of A_1
r = resonant states

Received December 20, 1972; revision received July 9, 1973.
Index categories: Radiatively Coupled Flows and Heat Transfer; Atomic, Molecular, and Plasma Properties; Radiation and Radiative Heat Transfer.

* Professeur à l'Université de Rouen.
† Maître-Assistant à l'Université de Rouen, détaché au C.E.A.
‡ Assistant à l'Université de Rouen.

I. Introduction

IN many studies on plasma-jets, electron-ion recombination rate coefficients of homogeneous decaying plasmas are often used in the species (electrons and ions) conservation equations.

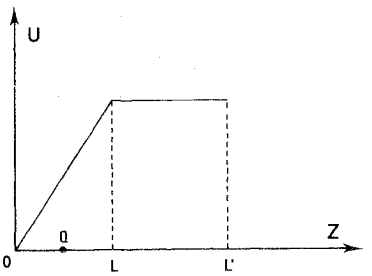

Fig. 1 Assumed velocity profile in boundary layer. Z is the distance normal to the wall, U is the velocity in the streamwise direction, and $L'-L$ = the thickness of the homogeneous plasma.

It is now well-known[1,3] that this rate is notably influenced by the depopulation rate of the metastable and resonant levels; thus, the recombination rate, at a point of the plasma, cannot be determined without resolving the resonance radiative transfer equation.

Holstein[4] studied the resonance radiative transport for plasmas which are homogeneous except in the case where the population density of resonant levels varies. Recently several authors[3,5-8] proposed numerical methods in order to determine the source function. Cogley[5] treated the problem of radiative transport for Lorentz profiles lines in nonisothermal gases. Avrett[3] treated it in the general case. Calculations of the line source function that include the effects of velocity gradients have been carried out in Refs. 6–8.

The aim of this work is to propose an approximate analytical solution of the transfer equation. When the velocity is not uniform, it is obvious that the resonance radiative transport depends upon velocity gradients, since, if we consider the line profiles for an emitting atom at one point in the gas and for an abosrbing atom at another point, there is a doppler shift of the line. If we want to take into account all the gradients of physical parameters (density, kinetic temperature of heavy particles, electronic density, velocity...) which have an influence upon the line profile, we obtain a very complex system of equations. We shall content ourselves with studying plasmas which are homogeneous except for variation in velocity and in the population densities of the resonant levels. Therefore, our work will have a practical interest in the case of low-pressure supersonic plasma-jets and of a boundary layer on a plate in a low pressure supersonic flow.[9,10]

The paper is organized as follows. In Secs. II and III are given the assumptions, the equations, and their transformation in a more useful form. In Secs. IV and V, the equations giving the radiative population rate of the resonant levels are resolved. Section IV deals with the population rate due to radiation coming from the boundary-layer plasma and Sec. V deals with the radiation coming from the freestream plasma. In our conclusions, we give the manner of using our results.

II. Resonance Radiative Transfer Equations

We simplify the problem by supposing that the velocity profile is linear in the boundary layer (thickness L) and the flow patterns, parallel to the wall (Fig. 1).

Let us evaluate the population rate, by absorption, per unit volume, of resonant levels: $(dN_r/dt)_{abs}$ at the point $Q(0,0,Z)$, with $0 < Z < L$ (Fig. 1). We translate the axes and take Q as the origin of axes ξ, η, ζ (Fig. 2). $(dN_r/dt)_{abs}$ consists of three terms coming from:

1) The fraction of radiation which is emitted by the zone $0 < \xi < l$ of the plasma, reaches Q, and is absorbed per unit volume at this point [we call Δ_+ the corresponding contribution to $(dN_r/dt)_{abs}$]; 2) the radiation coming from the zone $-Z < \zeta < 0$ and absorbed in Q [we call Δ the corresponding contribution to $(dN_r/dt)_{abs}$]; 3) the radiation absorbed in Q coming from the homogeneous layer, $\zeta \geq l$ [its contribution to $(dN_r/dt)_{abs}$ will be called B].

By supposing the resonance radiative diffusion to be isotropic (complete redistribution), we shall easily show that the expressions of Δ_+, Δ_- and B are

$$\Delta_+ = \int_{\xi=-\infty}^{+\infty}\int_{\eta=-\infty}^{\infty}\int_{\zeta=0}^{l}\int_{\nu=0}^{\infty}\left[\frac{1}{4\pi}\frac{N_r(M)\varepsilon_\nu(M)}{\tau}\right]\times \frac{\exp\left\{-\int_0^\zeta \frac{k_\nu(P)}{\cos\theta}dW\right\}}{\xi^2+\eta^2+\zeta^2}k_\nu(Q)\,d\xi\,d\eta\,d\zeta\,d\nu \quad (1)$$

$$\Delta_- = \int_{\xi=-\infty}^{+\infty}\int_{\eta=-\infty}^{+\infty}\int_{\zeta=-Z}^{0}\int_{\nu=0}^{\infty}\left[\frac{1}{4\pi}\frac{N_r(M)\varepsilon_\nu(M)}{\tau}\right]\times \frac{\exp\left\{-\int_0^\zeta \frac{k_\nu(P)}{\cos\theta}dW\right\}}{\xi^2+\eta^2+\zeta^2}k_\nu(Q)\,d\xi\,d\eta\,d\zeta\,d\nu \quad (2)$$

$$B = \int_{\xi=-\infty}^{+\infty}\int_{\eta=-\infty}^{+\infty}\int_{\nu=0}^{\infty}\left[\frac{I_\nu(l,\theta)}{h\nu}\frac{\cos\theta}{\xi^2+\eta^2+\zeta^2}\times \exp\left\{-\int_0^l \frac{k_\nu(P)}{\cos\theta}dW\right\}\right]k_\nu(Q)\,d\xi\,d\eta\,d\nu \quad (3)$$

In these expressions, $N_r(M)$ is the population density number of a resonance level at the point M

$$\varepsilon_\nu(M) = \frac{k_\nu(M)}{S} \text{ (see Holstein[4])}$$

$$S = \int_{\text{line}} k_\nu\,d\nu = B_{fr}N_f\frac{h\nu}{C} \text{ (induced emission is neglected)}$$

B_{fr} is the absorption transition probability and N_f, the ground-level density number

$$\tau = 1/A_{fr}$$

A_{fr} being the emission transition probability, $I_\nu(l,\theta)$ is the specific intensity at a point $\zeta = l$ of the homogeneous plasma, in the direction of Q.

The population rate of the resonance level by radiative transitions between this level and the ground level is given by

$$(dN_r/dt)_{f\rightleftarrows r} = \Delta_+ + \Delta_- + B - N_r/\tau \quad (4)$$

In the following study, we shall suppose that k_ν has a doppler profile. This hypothesis is valid[11,12] in the case of our experimentally studied plasmas[9,10] (argon plasma: pressure $\simeq$ 1 torr, kinetic temperature of heavy particles $\simeq$ 1000°K, electron density $\simeq 10^{14}$ electron/cm^3).

In these conditions, if we take the frequency at the center of the line to be ν_0 at the point Q, we have:

$$k_\nu(P) = k_\nu(w) = k_0 \times \exp\left\{-\alpha\left[\nu-\nu_0+\nu_0\frac{U(w)-U(0)}{C}\cdot\frac{\eta}{(\xi^2+\eta^2+\zeta^2)^{1/2}}\right]^2\right\}$$
$$k_\nu(Q) = k_\nu(w=0);\quad k_\nu(M) = k_\nu(w=\zeta) \quad (5)$$
$$\varepsilon_\nu(M) = k_\nu(M)/S$$

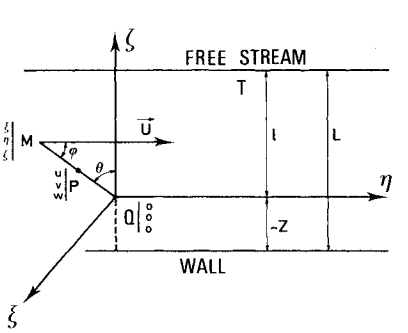

Fig. 2 Coordinate system.

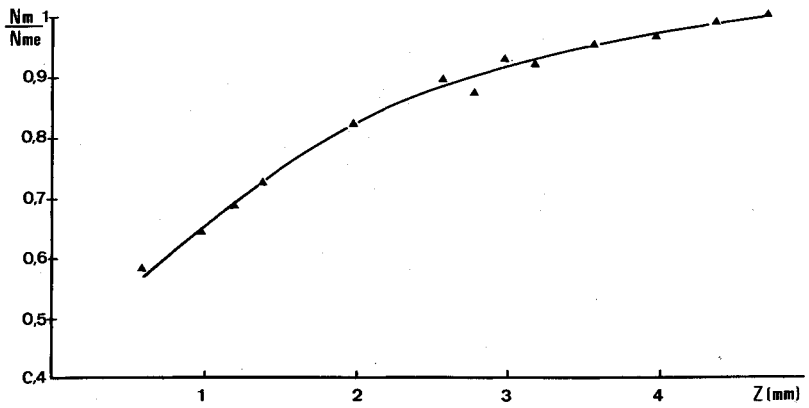

Fig. 3 Typical metastables ($1s_5$ of A_I) density profile[9] in a boundary layer along a flat plate. The characteristics of the used plasma are: electronic density = 10^{14} particles per cm^3; electronic temperature ≃ 7500°K; static pressure ≃ 1 torr − velocity ≃ 1000 m/sec.

and $\alpha = (1/\delta\nu_D)^2 = c^{te}$. $2\delta\nu_D$ is the doppler half width. According to the assumed hypothesis, $\delta\nu_D$ is a constant.

III. Transformation of Equations

Let us take θ, ϕ, ζ as new variables (cf. Fig. 2). We shall write

$$F(\nu, \zeta, \phi, \theta) = \exp\left\{-\int_0^{\zeta} \frac{k_\nu(w)}{\cos\theta}\, dw\right\}$$

and

$$\psi(\zeta) = N_r(M)/S$$

By taking into account the symmetries in the formulas, we can show rather easily that Δ_+, Δ_- and B can be written thus

$$\Delta_+ = -\frac{1}{\pi\tau}\int_0^{\pi/2}\int_{\phi=(\pi/2)-\theta}^{\pi/2}\int_{\zeta=0}^{l}\int_{\nu=0}^{\infty} \psi(\zeta)\frac{\partial F}{\partial\zeta}\times k_\nu(0)\Phi(\theta,\phi)\, d\phi\, d\theta\, d\zeta\, d\nu \quad (6)$$

$$\Delta_- = -\frac{1}{\pi\tau}\int_0^{\pi/2}\int_{\phi=(\pi/2)-\theta}^{\pi/2}\int_{\zeta=-Z}^{0}\int_{\nu=0}^{\infty} \psi(\zeta)\frac{\partial F}{\partial\zeta}\times k_\nu(0)\Phi(\theta,\phi)\, d\phi\, d\theta\, d\zeta\, d\nu \quad (7)$$

$$B(l) = 4\int_0^{\pi/2}\int_{\phi=(\pi/2)-\theta}^{\pi/2}\int_{\nu=0}^{\infty} k_\nu(0)\frac{I_\nu(l,\theta)}{h\nu}\times F(\nu,\theta,\phi,l)\Phi(\theta,\phi)\, d\phi\, d\theta\, d\nu \quad (8)$$

where

$$\Phi(\theta,\phi) = \sin\theta\sin\phi/(\sin^2\phi - \cos^2\theta)^{1/2}$$

In radiative transfer problems, it is usual to say that the values of the integrals, Δ_+ and Δ_-, are principally influenced by radiative transfers between layers close to the point Q, which impels us to replace $\psi(\zeta)$ by $\psi(0)$ in Δ_+ and Δ_- (zero approximation).

Drawin[2] contests such an attitude. However, we shall use this approximation but shall take the following precautions. 1) It is not necessary to calculate each of the terms Δ_+ and Δ_-. We just have to calculate their sum. 2) Figure 3 shows a typical profile of density of atoms in the $1s_5$ state (Paschen notation), in a boundary layer along a flat plate. This plate is put in a low pressure (1 torr) argon plasma flow.[9,10]. The electronic density number in the freestream is about 10^{14} particles/cm^3. The experimental points on Fig. 3 are obtained by near infrared (7635 Å) absorption measurements. The population density profile of metastable and resonant levels can be considered, to a close approximation, to be linear near the wall.

By taking into account this expression and the antisymmetry of the second term, we find that the zero approximation will be valid if we consider the radiative transfer to occur in the vicinity of points situated in the middle of the boundary layer. Thus we shall replace $\Delta_+ + \Delta_-$ by $\delta_+ + \delta_-$, δ being deducible from Δ by replacing $\psi(\zeta)$ by $\psi(0)$.

If we take into account Eq. (5), we can easily get the results after integration with respect to ζ

$$\delta_+ = N_r/2\tau - \beta(l)N_r/\pi\tau S; \quad \delta_- = N_r/2\tau - \beta(Z)N_r/\pi\tau S \quad (9)$$

where

$$\beta(Z) = \int_0^{\pi/2}\int_{\phi=(\pi/2)-\theta}^{\pi/2}\int_{\nu=0}^{\infty} k_\nu(0)\Phi(\phi,\theta)F(Z,\theta,\phi)\, d\phi\, d\theta\, d\nu \quad (10)$$

The problem is then reduced to the calculation of the β terms.

We can appreciate the physical sense of the following calculations more easily be reference to new axes (Fig. 4). The homogeneous zone is situated above the plane $\pi(Z = 0)$. Equations are thus written

$$k_\nu(Q) = k_\nu(l) = k_0(Q)\exp\{-\alpha[\nu - \nu_0' + \nu_0'\gamma l\cos\phi]^2\} \quad (11)$$

$$k_\nu(P) = k_\nu(w') = k_0(P)\exp\{-\alpha[\nu - \nu_0' - \nu_0'\gamma w'\cos\phi]^2\}$$

where ν_0' is the frequency at the center of the line of the homogeneous plasma.

As we have already indicated, we suppose the velocity profile to be linear in the zone $Z > 0$; that is, that $\gamma = -(1/C)\,\partial U/\partial z$ is supposed to be constant for $0 \leqq z \leqq U_e/C\gamma$, U_e being the freestream velocity. β will then be written

$$\beta(l) = \int_0^{\pi/2}\int_{\phi=(\pi/2)-\theta}^{\pi/2}\int_{\nu=0}^{\infty}\left[\frac{k_\nu(l)\sin\theta\sin\phi}{(\sin^2\phi - \cos^2\theta)^{1/2}}\times \exp\left\{-\int_0^{l}\frac{k_\nu(w')}{\cos\theta}\, dw'\right\}\right] d\phi\, d\theta\, d\nu \quad (12)$$

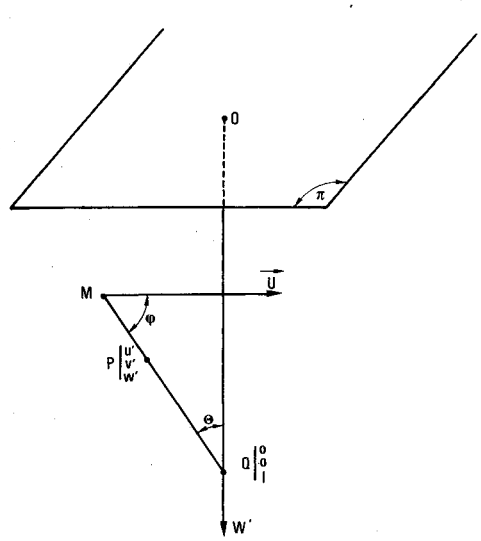

Fig. 4 New coordinate system (the freestream plasma is situated above the plane π).

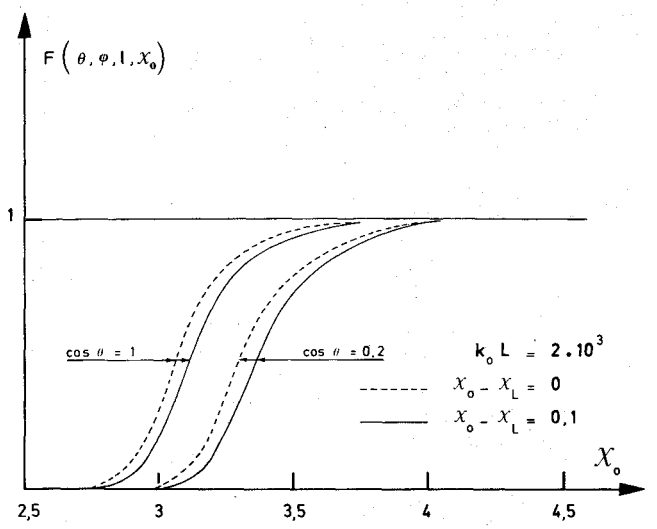

Fig. 5 Function $F(\theta, \phi, l, \chi_0)$ appearing in Sec. IV [Eq. (16)] (case of small gradient). The value of $k_0 l$ is assumed to be $= 2.10^3$. The dotted line is for the case $\chi_0 - \chi_l = 0$, and the full line for $|\chi_0 - \chi_l| = 0,1$.

It can then easily be shown that

$\beta(l) = -\partial\psi/\partial l$ where

$$\psi(l) = \int_0^{\pi/2} \int_{\phi=(\pi/2)-\theta}^{\pi} \frac{G(\theta\phi l)\cos\theta \sin\theta \sin\phi}{(\sin^2\phi - \cos^2\theta)^{1/2}} d\theta\, d\phi \qquad (13)$$

and

$$G(\theta, \phi, l) = \int_{v=0}^{\infty} F(v, \theta, \phi, l)\, dv$$

we define

$$\chi = (v - v_0' + v_0' \gamma w' \cos\phi)(\alpha)^{1/2} \text{ and } \chi_0 = (v - v_0')(\alpha)^{1/2} \qquad (14)$$

G is then obtained as:

$$G(\theta, \phi, l) = \frac{1}{(\alpha)^{1/2}} \int_{-\infty}^{+\infty} d\chi_0 \times \exp\left\{ - \frac{k_0}{(\cos\theta \cos\phi)\gamma v_0 (\alpha)^{1/2}} \int_{\chi_0}^{\chi_l} \exp(-\chi^2)\, d\chi \right\} \qquad (15)$$

Thus, the problem is now to calculate $G(\theta, \phi, l)$. Then $\beta(l)$ will be obtained by means of Eq. (13), and δ_+ and δ_-, by means of Eq. (9).

IV. Calculation of the β Term

Case 1 : When $v_0 \gamma l(\alpha)^{1/2}$ is Weak (Small Gradient)

According to Eq. (14), $v_0 \gamma l(\alpha)^{1/2}$ being weak is equivalent to $\chi_l - \chi_0$ being small.

If we expand

$$\int_{\chi_0}^{\chi_l} d\chi \exp(-\chi^2)$$

into a power series of $\chi_l - \chi_0$, we can write the following expression:

$$F(\theta, \phi, l, \chi_0) = \exp\left\{ - \frac{k_0}{(\cos\theta \cos\phi)\gamma v_0 (\alpha)^{1/2}} \times \exp\left[- \int_{\chi_0}^{\chi_l} \exp(-\chi^2)\, d\chi \right] \right\} = \exp\left\{ - \frac{k_0 l}{\cos\theta} \exp(-\chi_0^2) \times \left[1 - \chi_0(\chi_l - \chi_0) + \frac{2\chi_0^2 - 1}{3} (\chi_l - \chi_0)^2 + \cdots \right] \right\} \qquad (16)$$

Figure 5 shows the shape of the curve of F vs χ_0. We note that the curves can be deduced from one another by a translation along the χ_0 axis.

From the expression of $F(\theta, \phi, l, \chi_0)$, it can be shown that the shift, in relation to the curve corresponding to $\chi_l - \chi_0$, is given by $d = \chi_{om}' - \chi_{om}$. χ_{om}' and χ_{om} are related according to the following expression:

$$\exp(-\chi_{om}^2) = \exp\left\{ -\chi_{om}'^2 \left[1 - \chi_{om}'(\chi_l - \chi_0) + \frac{2\chi_{om}' - 1}{3} (\chi_l - \chi_0)^2 + \cdots \right] \right\}$$

χ_{om} and χ_{om}' are the values which make $F(\theta, \phi, l = 0, \chi_0)$ and $F(\theta, \phi, l, \chi_0)$, respectively, equal to the same value, $\frac{1}{2}$ for example. We get

$$d \simeq -(\chi_l - \chi_0)/2 + (\chi_{om}/12)(\chi_l - \chi_0)^2 + \cdots \qquad (17)$$

Let d_+ be the shift of the curve of $F(\theta, \phi, l, \chi_0)$ versus χ_0 in relation to that of $F(\theta, \phi, l = 0, \chi_0)$ for the positive values of χ_0 and d_- be the shift corresponding to the negative values of χ_0, we get

$$\mu = d_+ - d_- = (\chi_{om}/6)(\chi_l - \chi_0)^2 (\chi_{om} > 0) \qquad (18)$$

Concerning the integration of F with respect to χ_0 to get G, it is now obvious that the variations with l of the area between the curve $F(\theta, \phi, \chi_0, l)$ and the χ_0 axis (Fig. 5) will easily be expressed vs μ.

Let us take Eqs. (13–15) into account and write

$$\beta(l) = -\int_0^{\pi/2} \int_{\phi=(\pi/2)-\theta}^{\pi/2} \frac{1}{(\alpha)^{1/2}} \frac{\partial\mu}{\partial l} \frac{\cos\theta \sin\theta \sin\phi}{(\sin^2\phi - \cos^2\theta)^{1/2}} d\phi\, d\theta + \beta_0(l) \qquad (19)$$

where $\beta_0(l)$ is the value of $\beta(l)$ corresponding to $\gamma = 0$ (no velocity gradient), which will be calculated further.

Readers are reminded that χ_{om} is defined by

$$(k_0 l/\cos\theta) \cdot \exp(-\chi_{om}^2) = \log 2$$

from which we get

$$\partial\chi_{om}/\partial l = 1/2\chi_{om} l$$

And according to Eq. (18)

$$\partial\mu/\partial l = l[v_0 \gamma(\alpha)^{1/2} \cos\phi]^2 [\chi_{om}/3 + 1/12\chi_{om}] \qquad (20)$$

Since χ_{om} is greater than 3 in the practical case that we shall study, it is seen that the preceding expression may be written

$$\partial\mu/\partial l = l(v_0 \gamma(\alpha)^{1/2} \cos\phi)^2 (\chi_{om}/3) \qquad (20)$$

Thus, it now remains to integrate $\beta(l)$ [Eq. (19)] by taking into account Eq. (20) and the expression of χ_{om}

$$\chi_{om} = [\log k_0 l - \log(\cos\theta \log 2)]^{1/2}$$

To integrate $\beta(l)$, we can neglect $\log(\cos\theta \log 2)$ which varies from 0.3 to 3 when $\cos\theta$ varies from 1 to $\frac{1}{20}$, while $\log k_0 l$ ranges about a value of 9 in the proposed application. The integration is then easy and leads to

$$\beta(l) - \beta_0(l) = (\pi/48) v_0^2 \gamma^2 (\alpha)^{1/2} l (\log k_0 l)^{1/2} \qquad (21)$$

When l varies, the curves of $\exp\{-k_0 l \exp(-\chi_0^2)\}$ vs χ_0 can be deduced by translation along the χ_0 axis. The corresponding shift is equal to the variation of χ_{om}, where χ_{om} is given by

$$k_0 l \exp(-\chi_{om}^2) = C^{te} = \log 2 \qquad (22)$$

Proceeding in the same manner for the calculation of $G(\theta, \phi, l)$, which is written

$$G(\theta, \phi, l) = \frac{1}{(\alpha)^{1/2}} \int_{-\infty}^{+\infty} \exp\{-k_0 l \exp(-\chi_0^2)\}\, d\chi_0 \qquad (23)$$

we shall first calculate the quantity $\mu_0 = 2\chi_{om}$ corresponding to the value of μ given in Eq. (18). Then, $\partial\mu_0/\partial l = 2\,\partial\chi_{om}/\partial l$; that is, according to Eq. (22),

$$\frac{\partial\mu_0}{\partial l} = \frac{1}{l\chi_{om}} = \frac{1}{l(\log k_0 l - \log\log 2)^{1/2}} \neq \frac{1}{l(\log k_0 l)^{1/2}} \qquad (24)$$

and we can find

$$\beta_0(l) = [\pi/4l(\alpha)^{1/2}]\, 1/(\log k_0 l)^{1/2} \qquad (25)$$

This result will also be found by proceeding as shown by

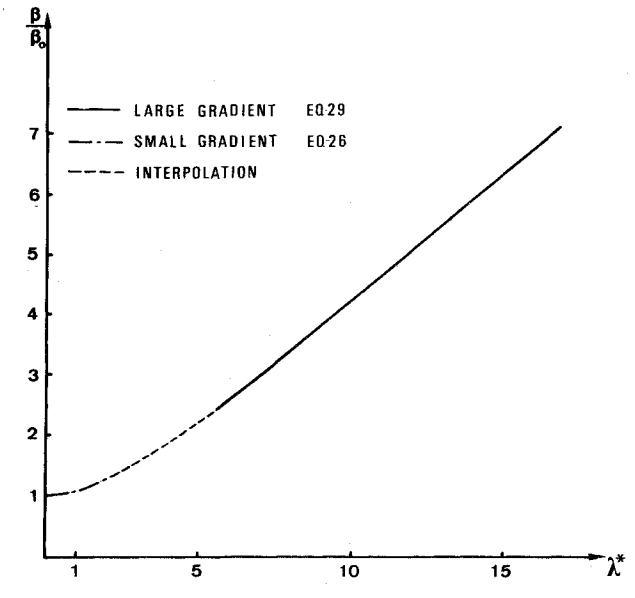

Fig. 6 Influence of the velocity gradient upon the coefficient β/β_0. $\lambda = l$ or Z; $\lambda^* = v_0\gamma(\alpha)^{1/2}\lambda(\log k_0\lambda)^{1/2}$ (dimensionless length).

Holstein.[4] Thus, in the case of small gradients the ration β/β_0 is given by the relationships

$$\beta(\lambda)/\beta_0(\lambda) = 1 + \lambda^{*2}/12 \tag{26}$$

where $\lambda = l$ or Z and $\lambda^* = v_0\gamma\lambda(\alpha)^{1/2}(\log k_0 l)^{1/2}$ (dimensionless length). Figure 6 shows the variation of the ratio β/β_0 vs λ^*.

Case 2: When $v_0\gamma l(\alpha)^{1/2}$ is Large

We define

$$a = k_0/(\cos\theta\cos\phi)v_0\gamma(\alpha)^{1/2}$$

Equation (15) is then written

$$G(\theta,\phi,l) = \frac{1}{(\alpha)^{1/2}}\int_0^{\infty} d\chi_0 \exp\left\{-a\int_{\chi_0}^{+\infty}\exp(-\chi^2)\,d\chi\right\}\times \exp\left\{-a\int_{\infty}^{\chi_l}\exp(-\chi^2)\,d\chi\right\} + \frac{1}{(\alpha)^{1/2}}\int_{-\infty}^{0} d\chi_0 \times \exp\left\{-a\int_{\chi_0}^{-\infty}\exp(-\chi_2)\,d\chi\right\}\exp\left\{-a\int_{-\infty}^{\chi_l}\exp(-\chi^2)\,d\chi\right\} \tag{27}$$

In the integration with respect to χ_0 for the calculation of $G(\theta,\phi,l)$, we only take into account the values of $|\chi_0|$ for which

$$\exp\left\{-a\int_{\chi_0}^{\infty}\exp(-\chi^2)\,d\chi\right\}$$

is not extremely small, that is for $|\chi_0|$ great enough (in the practical applications).

Writing $\chi = \chi_0(1+x)$, we get

$$\int_{\chi_0}^{\infty}\exp(-\chi^2)\,d\chi \simeq \int_0^{\infty}\chi_0\exp\{-\chi_0^2(1+2x)\}\,dx = \frac{1}{2\chi_0}\exp(-\chi_0^2)$$

and since $\chi - \chi_0$ is supposed to be great, we get

$$\int_{\chi_l}^{\infty}\exp(-\chi^2)\,d\chi = \frac{\exp(-\chi_l^2)}{2\chi_l} = \frac{\exp\{-[\chi_0 + v_0 l\gamma(\alpha)^{1/2}\cos\phi]2\}}{2[\chi_0 + v_0 l\gamma(\alpha)^{1/2}\cos\phi]}$$

In Fig. 7, it can be noted that 1) the curve of $\exp\{-(a/2\chi_0)\exp(-\chi_0^2)\}$ is still practically parallel to that of $\exp\{-a\exp(-\chi_0^2)\}$, and 2) the first term of $G(\theta,\phi,l)$ appearing in Eq. (27) may be written

$$\int_0^{\infty}\exp\left\{-a\int_{\chi_0}^{\infty}\exp(-\chi^2)\,d\chi\right\}d\chi_0$$

this expression being independant of l.

Indeed, for the positive values of χ_0, the contribution to $G(\theta,\phi,l)$ of the values of $\chi_0 < 2$ is negligible, and, for $\chi_0 > 2$,

$$\exp\left\{-a\int_{\infty}^{\chi_l}\exp(-\chi^2)\,d\chi\right\} \simeq 1$$

For the values of $\chi_0 > 0$, the second term of Eq. (27) is practically equal to zero. On the contrary, for the negative values of χ_0, the first term of Eq. (27) is practically equal to zero and only the second term remains.

By proceeding as before, it will be shown (cf., Fig. 7) that, for $\chi_0 < 0$, $G(\theta,\phi,l)$ is practically equal to

$$\frac{1}{(\alpha)^{1/2}}\int_{-\infty}^{0}\exp\left\{\frac{a\exp\{-[\chi_0 v_0\gamma l(\alpha)^{1/2}\cos\phi]^2\}}{2(\chi_0 + v_0\gamma l(\alpha)^{1/2}\cos\phi)}\right\}d\chi_0$$

It will be noted that, for $\chi_0 < 0$, the curve of the variations of

$$\exp\left\{\frac{a\exp\{-[\chi_0 + v_0\gamma l(\alpha)^{1/2}\cos\phi]^2\}}{2[\chi_0 + v_0\gamma l(\alpha)^{1/2}\cos\phi]}\right\}$$

vs χ_0 can pratically be deduced from the curve of

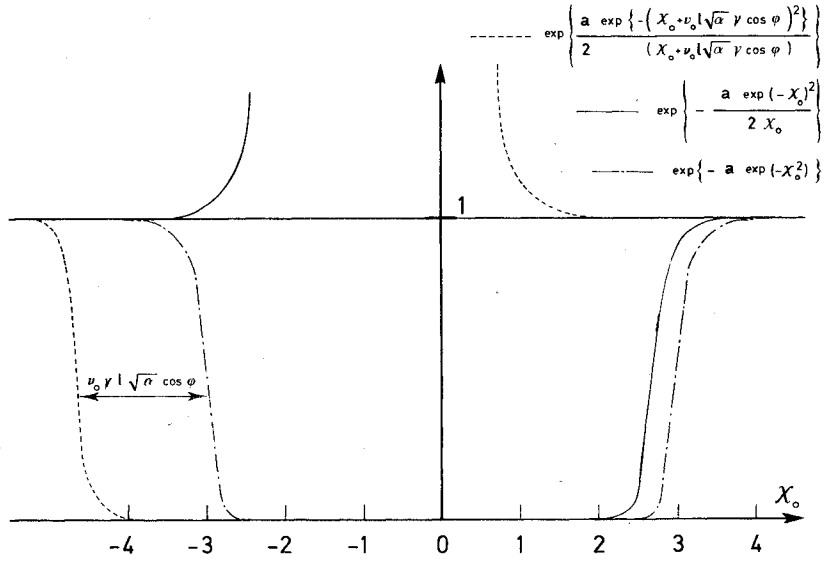

Fig. 7 Functions appearing in Sec. IV (case of large gradient).

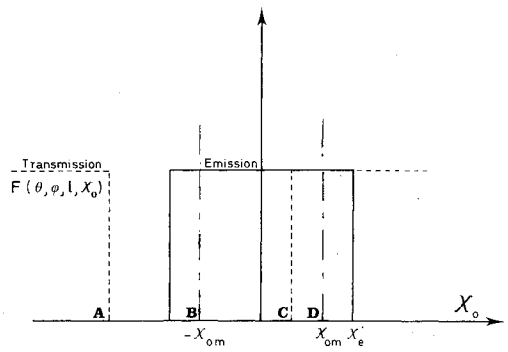

Fig. 8 Assumed profiles for emission (full line) and transmission (dotted line).

$\exp[-a\exp(-\chi_0{}^2)]$ by a translation along the χ_0-axis [its length is practically equal to $v_0\gamma l(\alpha)^{1/2}\cos\phi$].

Then the equivalent of Eq. (18) may be written

$$\mu = d_+ - d_-$$

where d_+ does not depend on l and $d_- = v_0 l\gamma(\alpha)^{1/2}\cos\phi$. So $\partial\mu/\partial l = -v_0\gamma(\alpha)^{1/2}\cos\phi$.

If we subsitute these values into Eq. (13), we get

$$\beta(l) = v_0\gamma/3 \tag{28}$$

The latter result may be got more strictly (see C.E.A. Report[13]). Thus, in the case of large gradients, the ratio β/β_0 is given by the relationship

$$\beta(\lambda)/\beta_0(\lambda) = (4/3\pi)\lambda^* \text{ (see Fig. 6)} \tag{29}$$

where $\lambda = l$ or Z, $\lambda^* = v_0\gamma\lambda(\alpha)^{1/2}(\log k_0 l)^{1/2}$ (dimensionless length).

The results obtained in this section are summed up in Fig. 6. We plot as the abscissa the dimensionless length λ^*, this quantity being directly proportional to the gradient of the Mach number. For the small values of the velocity gradient, β must be calculated by means of Eq. (21). For the large values of the velocity gradient, β is given by Eq. (28). We are now able to calculate $\Delta_+ + \Delta_- = \delta_+ + \delta_-$ [see Eq. (9)].

V. Calculation of B

Case 1: When the Thickness l' of the Homogeneous Plasma is Much Greater than l

We shall suppose l' to be much greater than the thickness l of the region where the velocity gradient exists and take the index e for the parameters corresponding to the homogeneous area (freestream in the case of a boundary layer).

In such conditions, over a large frequency range, the specific intensity $I_\nu(l, \theta)$ of the homogeneous plasma in $Z = 0$ may be replaced by the Planck function $I_\nu{}^0(T_{ex})_e$ where $(T_{ex})_e$ is the relative excitation temperature of the resonance and ground levels in the homogeneous area and is given by

$$(T_{ex})_e = \frac{-E_r}{k\log|N_r/N_f|_e g_f/g_r} \tag{30}$$

Taking into account the Einstein relations and equations (3, 10, and 30), we can write

$$B(l) = \beta(l)N_{re}/\pi\tau s \tag{31}$$

We now note that the results of Secs. III and IV and Eqs. (9) and (31) allow us to express Eq. (4) as

$$\left(\frac{dN_r}{dt}\right)_{f\rightleftarrows r} = \frac{1}{\pi\tau s}\{\beta(l)N_{re} - [\beta(l)+\beta(z)]N_r\} \tag{32}$$

Case 2: When the Thickness l' of the Homogeneous Plasma May Have any Value

We now shall consider the situation where l' has any value and we shall show that supposing that $I_\nu(l, \theta)$ is constant over a large frequency range is not a realistic hypothesis Indeed, in highly supersonic flows, $v_0\gamma(\alpha)^{1/2}l$ may be great ($\simeq 10$ and more). Let us study this case.

We noted previously that photons whose frequency was greater than ν_0 ($\chi > 0$) do not contribute to the calculation of $\beta(l)$.

For the negative values of χ, as a first approximation, we can replace the real emission profile by the rectangular profile drawn on Fig. 8 (full line). Its half-breadth $|\chi_e'(\theta)|$ is equal to

$$|\chi_e'(\theta)| \simeq (\log k_0 l' - \log\cos\theta)^{1/2} \simeq (\log k_0 l')^{1/2} = |\chi_e'|$$

The transmission curve (Fig. 8) of the plasma included between the plane π and Q (Fig. 4), that is, the curve of the variations of $F(\theta, \phi, l, \chi_0)$ vs χ_0 [Eq. (15)] may also be replaced by a step-function (dotted line in Fig. 8) as a first approximation.

This step-function begins at $\chi = \chi_e(\theta, \phi)$. According to Sec. V, the value of $\chi(\theta, \phi)$ is given by

$$|\chi_e(\theta, \phi)| = |\chi_{om}(\theta, \phi)| + v_0\gamma l(\alpha)^{1/2}\cos\phi \tag{33}$$

where

$$\chi_{om}(\theta, \phi) = -[\log k_0 l - \log\cos\theta - \log|v_0\gamma l(\alpha)^{1/2}\cos\phi| \times |2\chi_{om} + v_0\gamma l(\alpha)^{1/2}\cos\phi|]^{1/2} \tag{34}$$

In fact, the variations of χ_e vs ϕ are very distinctly more sensible to the variations of $v_0\gamma(\alpha)^{1/2}l\cos\phi$ than to the variations of $\lambda_{om}(\theta, \phi)$ vs ϕ. In such conditions Eqs. (33) and (34) may be simplified and we can write

$$|\chi_e| \simeq |\chi_{om}| + v_0\gamma l(\alpha)^{1/2}\cos\phi$$

where

$$|\chi_{om}| = (\log k_0 l)^{1/2}$$

Therefore, to suppose the specific intensity of the homogeneous plasma emission line constant between the limits of the integral is not a realistic hypothesis at all, since it amounts to supposing that

$$|\chi_e'| > \chi_{om} + v_0\gamma l(\alpha)^{1/2}$$

or

$$(\log k_0 l')^{1/2} > (\log k_0 l)^{1/2} + v_0\gamma(\alpha)^{1/2}l$$

which leads us to a thickness of the homogeneous plasma which is unrealistically too large when the Mach number increases. In fact, in practical cases, $\chi_e' - \chi_{om}$ is rather small and it is better to use the results found in the calculation of the β terms, when $v_0\gamma l(\alpha)^{1/2}$ is small (Sec. IV).

The homogeneous plasma emission profile at the limit of the boundary layer is replaced by the rectangular profile drawn on Fig. 9 (full line); its center is at $\chi_0 = 0$ and its width is χ_e'.

The inhomogeneous plasma transmission profile $F(\theta, \phi, l, \chi_0)$,

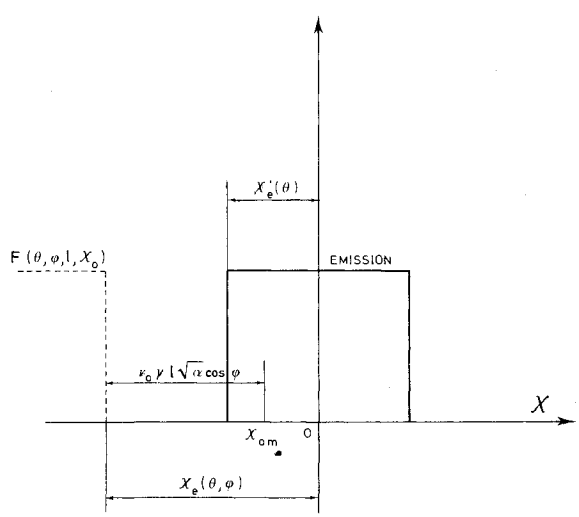

Fig. 9 Assumed profiles for emission (full line) and transmission (dotted line).

whose expression is given by relationship (16), is replaced by the dotted line which we can see on Fig. 9. AB is equal to

$$v_0\gamma(\alpha)^{1/2}l\cos\phi/2+(\chi_{om}/12)[v_0\gamma l(\alpha)^{1/2}\cos\phi]^2$$

CD is equal to

$$v_0\gamma(\alpha)^{1/2}l\cos\phi/2-(\chi_{om}/12)[v_0\gamma l(\alpha)^{1/2}\cos\phi]^2$$

[cf. relationship (17)].

Now, the problem is to know how to modify Eqs. (10, 13, and 31) to get the population rate term (per unit volume) of the resonance levels by absorption of the photons directly coming from the homogeneous zone. We shall now call this term $B'(l)$; it is always given by an expression like [Eq. (31)]

$$B'(l) = (N_{re}/\pi\tau S_e)\beta'(l) \tag{35}$$

But the expression of $\beta'(l)$ is different from that of $\beta(l)$; using Eq. (10), we obtain

$$\beta'(l) = \int_0^{\pi/2}\int_{\phi=(\pi/2)-\theta}^{\pi/2}\int_{-v_e'}^{v_e'}\left[\frac{k_\nu(l)\sin\theta\sin\phi}{(\sin^2\phi-\cos^2\theta)^{1/2}}\times \exp\left\{-\int_0^l\frac{k_\nu(w)}{\cos\theta}dw\right\}\right]d\phi\,d\theta\,d\nu \tag{36}$$

where v_e' is given by

$$\chi_e' = (v_e'-v_0)(\alpha)^{1/2}$$

The limits on the values of θ and ϕ will be studied later.

By making calculations like those made in Sec. IV we obtain

$$\beta'(l) = \frac{1}{(\alpha)^{1/2}}\int_0^{\pi/2}\int_{\phi=(\pi/2)-\theta}^{\pi/2}\frac{\cos\theta\sin\theta\sin\phi}{(\sin^2\phi-\cos^2\theta)^{1/2}}d\phi\,d\theta\times \int_{-\chi_e'}^{\chi_e'}\frac{\partial}{\partial l}H(\theta,\phi,l,\chi_0)\,d\chi_0 \tag{37}$$

where

$$H(\theta,\phi,l,\chi_0) = \exp\left[\frac{-k_0}{(\cos\theta\cos\phi)\gamma v_0(\alpha)^{1/2}}\times \exp-\left\{\int_{\chi_0}^{\chi_l}\exp(-\chi^2)\,d\chi\right\}\right]$$

Let us first take into account the negative values of χ_0. It is obvious (cf. Fig. 9) that only the values of ϕ for which

$$\chi_{om}+\frac{v_0\gamma(\alpha)^{1/2}l}{2}\cos\phi+\frac{\chi_{om}}{12}[v_0\gamma l(\alpha)^{1/2}\cos\phi]^2 \leqq \chi_e'$$

contribute to the calculation of $\beta'(l)$.

Let us call ϕ_2 the solution ($0 \leqq \phi_2 \leqq \pi/2$) of the equation

$$\chi_{om}+[v_0\gamma(\alpha)^{1/2}l/2]\cos\phi+(\chi_{om}/12)[v_0\gamma l(\alpha)^{1/2}\cos\phi]^2 = \chi_e'$$
$$\chi_e'-\chi_{om} = (\log k_0 l')^{1/2}-(\log k_0 l)^{1/2} \tag{38}$$

Only the values of ϕ greater than ϕ_2 contribute to the calculation of $\beta'(l)$.

Let us take into account our approximations and still use the same method as in Sec. IV. We can write, by calling $\beta_-'(l)$ the contribution to $\beta'(l)$ of the negative values of χ_0

$$\beta_-'(l) = \frac{1}{(\alpha)^{1/2}}\int_{\theta=(\pi/2)-\phi_2}^{\pi/2}\int_{\phi_2}^{\pi/2}\frac{\partial(d_-+\mu_0/2)}{\partial l}\times \frac{\cos\theta\sin\theta\sin\phi}{(\sin^2\phi-\cos^2\theta)^{1/2}}d\phi\,d\theta+\frac{1}{(\alpha)^{1/2}}\times \int_{\theta=0}^{(\pi/2)-\phi_2}\int_{\phi=(\pi/2)-\theta}^{\pi/2}\frac{\partial(d_-+\mu_0/2)}{\partial l}\times \frac{\cos\theta\sin\theta\sin\phi}{(\sin^2\phi-\cos^2\theta)^{1/2}}d\phi\,d\theta \tag{39}$$

The first term corresponds to the values of θ for which $\theta > \pi/2-\phi_2$ and the second one to the values of θ for which $\theta < \pi/2-\phi_2$.

Let us call the reader's attention to the meaning of d_- and μ_0

$$d_- = [v_0\gamma l(\alpha)^{1/2}/2]\cos\phi+(\chi_{om}/12)[v_0\gamma(\alpha)^{1/2}\cos\phi]^2$$
$$\chi_{om} \simeq (\log k_0 l)^{1/2}$$

and

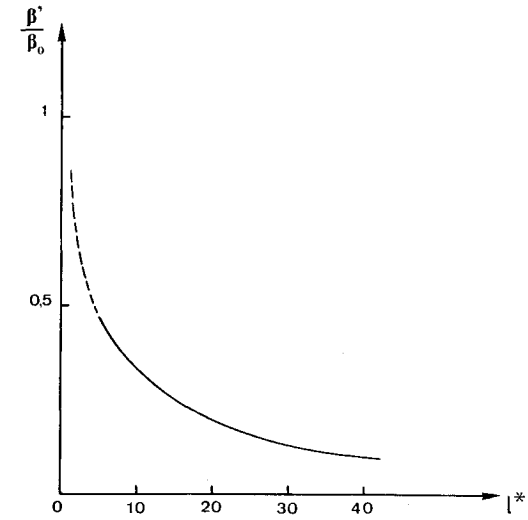

Fig. 10 Influence of the velocity gradient upon the ratio β'/β_0. l^* is the dimensionless length $l^* = v_0\gamma(\alpha)^{1/2}l(\log k_0 l)^{1/2}$. To plot this curve the values $l \simeq 1$ cm, $l' \simeq 5$ cm, $k_0 = 2.10^3$ have been assumed.

$$\mu_0 = 2\chi_{om}$$

If we use Eqs. (17–20) on the one hand and Eq. (24) on the other hand, the integration of Eq. (37) then gives

$$\frac{\beta'(l)}{\beta_0(l)} = \frac{2}{\pi}\left[\frac{\pi}{4}\sin^2\phi_2-\frac{\phi_2}{2}+\frac{\sin^2\phi_2}{4}\right]+\frac{2}{3\pi}l^*\cos^3\phi_2+\frac{l^{2*}}{3\pi}\left[\frac{1}{8}\left(\frac{\pi}{2}-\phi_2\right)+\frac{1}{32}\sin^4\phi_2\right] \tag{40}$$

where ϕ_2 is given by

$$\cos\phi_2 = (3/l^*)\left(\left\{1+\tfrac{4}{3}(\log k_0 l)^{1/2}[(\log k_0 l')^{1/2}-(\log k_0 l)^{1/2}]\right\}^{1/2}-1\right)$$

(The assumption of large gradients yields: $l^* \gg 1$.)

Let us now calculate the contribution to $\beta'(l)$ of the positive values of χ_0 which we call $\beta_+'(l)$. In this case, the profile of $H(\theta,\phi,l,\chi_0)$ goes from 0 to 1 (cf. Fig. 9) for values of $\chi_0 < \chi_{om} < \chi_e$.

Here, there is no lower limit like ϕ_2. In fact, we shall see that it is fitting to consider only the values of ϕ greater than a limit ϕ_2' which we are going to determine. Indeed, in Sec. IV, we noted that, when $v_0\gamma(\alpha)^{1/2}l\cos\phi$ is great, the photons whose frequency is $\nu > \nu_0'$, ($\chi_0 > 0$), do not contribute to the population rate of resonance levels.

The lower limit ϕ_2' will be the value of ϕ for which the derivative of the following quantity with respect to l is equal to zero (cf. Fig. 9):

$$\chi_{om}-v_0\gamma l(\alpha)^{1/2}\cos\phi/2+(\chi_{om}/12)[v_0\gamma(\alpha)^{1/2}l\cos\phi]^2$$

which roughly gives

$$\cos\phi_2' = 3/l^*$$

After integration [Eq. (37)], we get

$$\frac{\beta_+'(l)}{\beta_0(l)} = \frac{2}{\pi}\left[\frac{\pi}{4}\sin^2\phi_2'-\frac{\phi_2'}{2}+\frac{\sin^2\phi_2'}{4}\right]-\frac{2}{3\pi}l^*\cos^3\phi_2'+\frac{l^{2*}}{3\pi}\left[\frac{1}{8}\left(\frac{\pi}{2}-\phi_2'\right)+\frac{1}{32}\sin^4\phi_2'\right] \tag{41}$$

where ϕ_2' is given by $\cos\phi_2' = 3/l^*$. (The assumption of large gradients yields $l^* \gg 1$.)

We finally get

$$\beta'((l)/\beta_0(l) = \beta_-'(l)/\beta_0(l)+\beta_+'(l)/\beta_0(l) \tag{42}$$

where $\beta_-'(l)/\beta_0(l)$ and $\beta_+'(l)/\beta_0(l)$ are given, respectively, by Eqs. (40) and (41).

We have plotted a curve of typical variations of the ratio $\beta'(l)/\beta_0(l)$ vs l^* in Figs. (10). This ratio appreciably decreases when the velocity gradient increases.

The balance Eq. (4) can be rewritten

$$(dN_r/dt)_{f\rightleftarrows r} = \delta_+ + \delta_- + B'(l) - N_r/\tau$$

According to Eqs. (9) and (35), we get

$$\left(\frac{dN_r}{dt}\right)_{f\rightleftarrows r} = \frac{1}{\pi\tau S}\{\beta'(l)N_{re} - |\beta(l)+\beta(z)|N_r\} \tag{43}$$

The expression of $\beta(l)$ and $\beta(z)$ is given by relationships (25, 26 and 29); that of $\beta'(l)$, by relationships (38, 40–42) (see Fig. 10).

As the velocity gradient increases, $\beta'(l)$ decreases whereas $\beta(l)$ and $\beta(z)$ increase and the ratio $\beta'(l)/[\beta(l)+\beta(z)]$ quickly decreases (Figs. 6 and 10).

For instance, in the case of argon (at low pressure) whose atom translation temperature is about 1000°K, the ratio $\beta'(l)/[\beta(l)+\beta(z)]$, which was about 1 in the case of a weak velocity gradient, finally ranges about 10^{-2} for a velocity gradient of 5000 m/sec/cm, which is not an extremely great gradient. It then becomes evident that the population and depopulation rates of the resonance levels, and hence, the creation or recombination rates of electrons are appreciably coupled with the velocity gradients.

VI. Conclusions

We have given an approximate analytical solution of the resonance radiative transfer equation for a plasma in which a velocity gradient exists. From the point of view of the reader it is sufficient to use Fig. 6, Eq. (43), and the end of Sec. V. It is then easy, in each experimental case, to evaluate the ratios β/β_0 (Fig. 6) and β'/β_0 and to draw a curve similar to that of Fig. 10. By looking at these curves one can see whether the resonance radiative transfer is influenced by the velocity gradient. An example given at the end of Sec. V shows this influence can be important in supersonic plasma flow.

Nevertheless one must keep in mind that the line profile has been assumed a doppler profile. Lorentz or Voigt profiles are smoother than doppler profiles. By the way, the influence of velocity gradients is less important than for doppler profile.

Let us remember finally that we have performed an approximate analytical solution. To get more precise results you have to use the numerical methods.[3,6-8]

References

[1] Drawin, H. W., "Validity Conditions for Local Thermodynamic Equilibrium," *Zeitschrift für Physik*, Vol. 228, 1969, pp. 99–119.

[2] Drawin, H. W., "Influence of Radiative Absorption on the Establishment of Local Thermodynamic Equilibrium," *Zeitschrift für Naturforschung*, Vol. 24a, 1969, p. 1492.

[3] Avrett, E. H., "Solution of Non-LTE Transfer Problems," *Journal of Quantitative Spectroscopy and Radiative Transfer*, Vol. 11, 1971, pp. 511–529.

[4] Holstein, T., "Imprisonment of Resonance Radiation in Gases," I–II, *Physical Review*, Vol. 72, No. 12, 1947, pp. 1212–1233 and Vol. 83, No. 6, 1951, pp. 1159–1168.

[5] Cogley, A. C., "Radiative Transport of Lorentz Lines in Non-isothermal Gases," *Journal of Quantitative Spectroscopy and Radiative Transfer*, Vol. 10, No. 9, 1970, pp. 1065–1075.

[6] Athay, R. G., "Velocity Effects on the Profiles of H_α and Two FeI Lines," *Solar Physics*, Vol. 12, 1970, p. 175.

[7] Hummer, D. G. and Rybicky, G. B., *Methods of Computational Physics*, Vol. 7, Academic Press, New York, 1967.

[8] Kulander, J. L., "Line Formation in a Differentially Moving Non-LTE Atmosphere," *Journal of Quantitative Spectroscopy and Radiative Transfer*, Vol. 8, 1968, p. 273.

[9] Valentin, P., Terrier, M., Vervisch, P., and Piar, G., "Laminar Boundary Layer in Low Pressure Argon Plasma," *Proceedings of the International Symposium on Dynamics of Ionized Gases*, University of Tokyo Press, Tokyo, Japan, 1971, pp. 207–221.

[10] Terrier, M. and Vervisch, P., "Etudes de couches limites dans un écoulement de plasma d'argon," Thèses 3ème cycle, Rouen, May 1971, Université de Rouen, Rouen, France.

[11] Breene, R. G., "Line Shape," *Review of Modern Physics*, Vol. 29, No. 1, Jan. 1957, pp. 94–143.

[12] Griem, H. R., *Plasma Spectroscopy*, McGraw-Hill, New York, 1964, pp. 63–101.

[13] Valentin, P. and Pinegre, M., "Influence des gradients de vitesse sur le transfert du rayonnement de résonance dans les jets de plasmas (cas de l'argon)," Rapport C.E.A.-D.A.M. 71-09 T.R.D.-DO 133, 1971, Commissariat à l'Energie Atomique, Sevran, France.